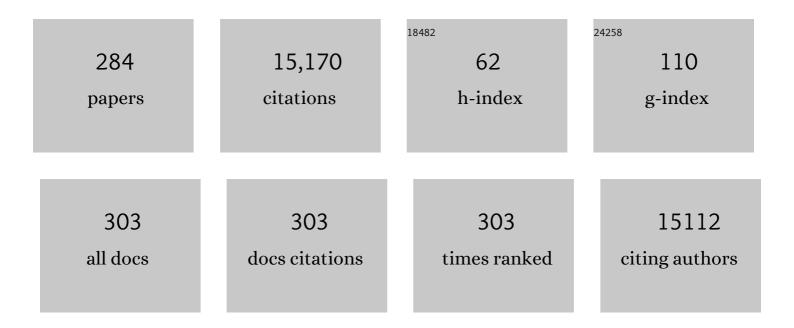
Robert E Lenkinski

List of Publications by Year in descending order

Source: https://exaly.com/author-pdf/1135212/publications.pdf Version: 2024-02-01



#	Article	IF	CITATIONS
1	Lactate Metabolism in Human Lung Tumors. Cell, 2017, 171, 358-371.e9.	28.9	899
2	Metabolic Heterogeneity in Human Lung Tumors. Cell, 2016, 164, 681-694.	28.9	830
3	PARACEST Agents:  Modulating MRI Contrast via Water Proton Exchange. Accounts of Chemical Research, 2003, 36, 783-790.	15.6	433
4	In vivo near-infrared fluorescence imaging of osteoblastic activity. Nature Biotechnology, 2001, 19, 1148-1154.	17.5	371
5	Primer on gadolinium chemistry. Journal of Magnetic Resonance Imaging, 2009, 30, 1240-1248.	3.4	335
6	Radio-Frequency Thermal Ablation with NaCl Solution Injection: Effect of Electrical Conductivity on Tissue Heating and Coagulation—Phantom and Porcine Liver Study. Radiology, 2001, 219, 157-165.	7.3	258
7	CEST: From basic principles to applications, challenges and opportunities. Journal of Magnetic Resonance, 2013, 229, 155-172.	2.1	257
8	Rotator cuff tears: diagnostic performance of MR imaging Radiology, 1989, 172, 223-229.	7.3	254
9	Clinical Utility of Proton Magnetic Resonance Spectroscopy in Characterizing Breast Lesions. Journal of the National Cancer Institute, 2002, 94, 1197-1203.	6.3	242
10	Prostate cancer: local staging with endorectal surface coil MR imaging Radiology, 1991, 178, 797-802.	7.3	224
11	Current role of MR imaging in the staging of adenocarcinoma of the prostate Radiology, 1993, 189, 339-352.	7.3	220
12	Human breast lesions: characterization with proton MR spectroscopy Radiology, 1998, 209, 269-275.	7.3	219
13	Prostate Cancer: Accurate Determination of Extracapsular Extension with High-Spatial-Resolution Dynamic Contrast-enhanced and T2-weighted MR Imaging—Initial Results. Radiology, 2007, 245, 176-185.	7.3	217
14	Prostate: MR imaging with an endorectal surface coil Radiology, 1989, 172, 570-574.	7.3	213
15	Gadolinium Retention: A Research Roadmap from the 2018 NIH/ACR/RSNA Workshop on Gadolinium Chelates. Radiology, 2018, 289, 517-534.	7.3	208
16	Proton magnetic resonance spectroscopy for detection of axonal injury in the splenium of the corpus callosum of brain-injured patients. Journal of Neurosurgery, 1998, 88, 795-801.	1.6	203
17	Interpretation of the pseudocontact model for nuclear magnetic resonance shift reagents. I. Agreement factor, R. Journal of the American Chemical Society, 1972, 94, 1742-1744.	13.7	188
18	A multicenter in vivo proton-MRS study of HIV-associated dementia and its relationship to age. Neurolmage, 2004, 23, 1336-1347.	4.2	180

#	Article	IF	CITATIONS
19	A concentration-independent method to measure exchange rates in PARACEST agents. Magnetic Resonance in Medicine, 2010, 63, 625-632.	3.0	176
20	Radiofrequency Ablation: Effect of Surrounding Tissue Composition on Coagulation Necrosis in a Canine Tumor Model. Radiology, 2004, 230, 761-767.	7.3	167
21	A systematic literature review of magnetic resonance spectroscopy for the characterization of brain tumors. American Journal of Neuroradiology, 2006, 27, 1404-11.	2.4	160
22	Gadolinium-Loaded Nanoparticles:  New Contrast Agents for Magnetic Resonance Imaging. Journal of the American Chemical Society, 2000, 122, 8940-8945.	13.7	153
23	The evaluation of human breast lesions with magnetic resonance imaging and proton magnetic resonance spectroscopy. Breast Cancer Research and Treatment, 2001, 68, 45-54.	2.5	153
24	Transient central nervous system white matter abnormality in X-linked Charcot-Marie-Tooth disease. Annals of Neurology, 2002, 52, 429-434.	5.3	150
25	Memantine and HIV-associated cognitive impairment: a neuropsychological and proton magnetic resonance spectroscopy study. Aids, 2007, 21, 1877-1886.	2.2	141
26	Renal perfusion in humans: MR imaging with spin tagging of arterial water Radiology, 1995, 196, 281-286.	7.3	139
27	MR imaging of the prostate at 3 tesla. Academic Radiology, 2004, 11, 857-862.	2.5	132
28	Body MR Imaging at 3.0 T: Understanding the Opportunities and Challenges. Radiographics, 2007, 27, 1445-1462.	3.3	127
29	Magnetization transfer imaging and proton MR spectroscopy in the evaluation of axonal injury: correlation with clinical outcome after traumatic brain injury. American Journal of Neuroradiology, 2001, 22, 143-51.	2.4	127
30	CEST and PARACEST MR contrast agents. Acta Radiologica, 2010, 51, 910-923.	1.1	123
31	Detection of Breast Cancer Microcalcifications Using a Dual-modality SPECT/NIR Fluorescent Probe. Journal of the American Chemical Society, 2008, 130, 17648-17649.	13.7	119
32	Proton MR spectroscopy of HIV-infected patients: characterization of abnormalities with imaging and clinical correlation Radiology, 1993, 186, 739-744.	7.3	116
33	Sodium MRI of the human kidney at 3 Tesla. Magnetic Resonance in Medicine, 2006, 56, 1229-1234.	3.0	116
34	Biochemical changes in the frontal lobe of HIV-infected individuals detected by magnetic resonance spectroscopy. Proceedings of the National Academy of Sciences of the United States of America, 1997, 94, 9854-9859.	7.1	115
35	Effects of anti-viral therapy and HCV clearance on cerebral metabolism and cognition. Journal of Hepatology, 2012, 56, 549-556.	3.7	115
36	Radiofrequency Ablation: Importance of Background Tissue Electrical Conductivity—An Agar Phantom and Computer Modeling Study. Radiology, 2005, 236, 495-502.	7.3	114

#	Article	IF	CITATIONS
37	Central gland and peripheral zone prostate tumors have significantly different quantitative imaging signatures on 3 tesla endorectal, in vivo T2â€weighted MR imagery. Journal of Magnetic Resonance Imaging, 2012, 36, 213-224.	3.4	112
38	Does Arterial Spin-labeling MR Imaging–measured Tumor Perfusion Correlate with Renal Cell Cancer Response to Antiangiogenic Therapy in a Mouse Model?. Radiology, 2009, 251, 731-742.	7.3	111
39	Elastic registration of multimodal prostate MRI and histology via multiattribute combined mutual information. Medical Physics, 2011, 38, 2005-2018.	3.0	100
40	Spectral detector CT-derived virtual non-contrast images: comparison of attenuation values with unenhanced CT. Abdominal Radiology, 2017, 42, 702-709.	2.1	96
41	Proton Magnetic Resonance Spectroscopy in the Frontal and Temporal Lobes of Neuroleptic Naive Patients with Schizophrenia. Neuropsychopharmacology, 1999, 20, 131-140.	5.4	93
42	Correlation of spectroscopy and magnetization transfer imaging in the evaluation of demyelinating lesions and normal appearing white matter in multiple sclerosis. Magnetic Resonance in Medicine, 1994, 32, 285-293.	3.0	90
43	Improved Coagulation with Saline Solution Pretreatment during Radiofrequency Tumor Ablation in a Canine Model. Journal of Vascular and Interventional Radiology, 2002, 13, 717-724.	0.5	89
44	A multi-center1H MRS study of the AIDS dementia complex: Validation and preliminary analysis. Journal of Magnetic Resonance Imaging, 2003, 17, 625-633.	3.4	88
45	Effects of Motor Cortex Modulation and Descending Inhibitory Systems on Pain Thresholds in Healthy Subjects. Journal of Pain, 2012, 13, 450-458.	1.4	87
46	Recent advances in magnetic resonance neurospectroscopy. Neurotherapeutics, 2007, 4, 330-345.	4.4	85
47	Filamin B mutations cause chondrocyte defects in skeletal development. Human Molecular Genetics, 2007, 16, 1661-1675.	2.9	83
48	Nuclear magnetic resonance studies of the denaturation of ubiquitin. Biochimica Et Biophysica Acta (BBA) - Protein Structure, 1977, 494, 126-130.	1.7	81
49	Magnetic Resonance Spectroscopy of Diffuse Brain Trauma in the Pig. Journal of Neurotrauma, 1998, 15, 665-674.	3.4	80
50	Magnetization Transfer Imaging of Diffuse Axonal Injury Following Experimental Brain Injury in the Pig: Characterization by Magnetization Transfer Ratio with Histopathologic Correlation. Journal of Computer Assisted Tomography, 1996, 20, 540-546.	0.9	80
51	Clinical effects and brain metabolic correlates in non-invasive cortical neuromodulation for visceral pain. European Journal of Pain, 2011, 15, 53-60.	2.8	79
52	Lactate production by human monocytes/macrophages determined by proton mr spectroscopy. Magnetic Resonance in Medicine, 1995, 34, 32-38.	3.0	75
53	Proton MRS and Neuropsychological Correlates in AIDS Dementia Complex: Evidence of Subcortical Specificity. Journal of Neuropsychiatry and Clinical Neurosciences, 2007, 19, 283-292.	1.8	75
54	On-target Inhibition of Tumor Fermentative Glycolysis as Visualized by Hyperpolarized Pyruvate. Neoplasia, 2011, 13, 60-71.	5.3	75

#	Article	IF	CITATIONS
55	Radiofrequency Ablation: Modeling the Enhanced Temperature Response to Adjuvant NaCl Pretreatment. Radiology, 2004, 230, 175-182.	7.3	73
56	Nephrogenic Systemic Fibrosis: A Chemical Perspective. Radiology, 2008, 247, 608-612.	7.3	72
57	High-Field Proton Magnetic Resonance Spectroscopy of a Swine Model for Axonal Injury. Journal of Neurochemistry, 2002, 70, 2038-2044.	3.9	69
58	3T MR of the prostate: Reducing susceptibility gradients by inflating the endorectal coil with a barium sulfate suspension. Magnetic Resonance in Medicine, 2007, 57, 898-904.	3.0	68
59	Magnetic resonance imaging of the brain: Blood partition coefficient for water: Application to spin-tagging measurement of perfusion. Journal of Magnetic Resonance Imaging, 1996, 6, 363-366.	3.4	67
60	Colorectal tumors: an in vitro study of high-resolution MR imaging Radiology, 1990, 177, 695-701.	7.3	65
61	Determinations of prostate volume at 3-tesla using an external phased array coil. Academic Radiology, 2003, 10, 846-853.	2.5	65
62	1H magnetic resonance spectroscopy characterization of neuronal dysfunction in drug-neive, chronic schizophrenia. Academic Radiology, 1994, 1, 211-216.	2.5	64
63	MRI detection of paramagnetic chemical exchange effects in mice kidneys in vivo. Magnetic Resonance in Medicine, 2007, 58, 650-655.	3.0	64
64	MR Neurography of Brachial Plexus at 3.0 T with Robust Fat and Blood Suppression. Radiology, 2017, 283, 538-546.	7.3	64
65	Exposure to Lead Appears to Selectively Alter Metabolism of Cortical Gray Matter. Pediatrics, 2001, 107, 1437-1442.	2.1	63
66	Breathhold abdominal and thoracic proton MR spectroscopy at 3T. Magnetic Resonance in Medicine, 2003, 50, 461-467.	3.0	63
67	New Magnetic Resonance Imaging Techniques for the Evaluation of Traumatic Brain Injury. Journal of Neurotrauma, 1995, 12, 573-577.	3.4	62
68	Pulmonary Perfusion: Respiratory-triggered Three-dimensional MR Imaging with Arterial Spin Tagging—Preliminary Results in Healthy Volunteers. Radiology, 1999, 212, 890-895.	7.3	62
69	Radiofrequency Tumor Ablation: Insight into Improved Efficacy Using Computer Modeling. American Journal of Roentgenology, 2005, 184, 1347-1352.	2.2	61
70	Determining histology-MRI slice correspondences for defining MRI-based disease signatures of prostate cancer. Computerized Medical Imaging and Graphics, 2011, 35, 568-578.	5.8	61
71	Quantitative comparison of magnetic resonance imaging (MRI) and histologic analyses of focal ischemic damage in the rat. Brain Research Bulletin, 1991, 26, 285-291.	3.0	60
72	A multislice gradient echo pulse sequence for CEST imaging. Magnetic Resonance in Medicine, 2010, 63, 253-256.	3.0	59

#	Article	IF	CITATIONS
73	Near-infrared fluorescence imaging of microcalcification in an animal model of breast cancer1. Academic Radiology, 2003, 10, 1159-1164.	2.5	57
74	On-resonance low B1 pulses for imaging of the effects of PARACEST agents. Journal of Magnetic Resonance, 2005, 176, 54-63.	2.1	54
75	pH imaging of mouse kidneys in vivo using a frequencyâ€dependent paraCEST agent. Magnetic Resonance in Medicine, 2016, 75, 2432-2441.	3.0	54
76	1H Spectroscopy without Solvent Suppression: Characterization of Signal Modulations at Short Echo Times. Journal of Magnetic Resonance, 2001, 153, 203-209.	2.1	53
77	Deuteration of a molecular probe for DNP hyperpolarization – a new approach and validation for choline chloride. Contrast Media and Molecular Imaging, 2011, 6, 499-506.	0.8	53
78	MR proton spectroscopy in multiple sclerosis. American Journal of Neuroradiology, 1992, 13, 1535-43.	2.4	53
79	Strategies for shimming the breast. Magnetic Resonance in Medicine, 2005, 54, 1139-1145.	3.0	51
80	Interpretation of the pseudocontact model for nuclear magnetic resonance shift reagents. IV. Evaluation of lanthanide-induced carbon-13 contact vs. pseudocontact nuclear magnetic resonance shifts. Journal of the American Chemical Society, 1973, 95, 3389-3390.	13.7	50
81	3 Tesla magnetic resonance imaging of the prostate with combined pelvic phased-array and endorectal coils. Academic Radiology, 2004, 11, 863-867.	2.5	49
82	Aqueous shift reagents for high-resolution cationic nuclear magnetic resonance. 2. Magnesium-25, potassium-39, and sodium-23 resonances shifted by chelidamate complexes of dysprosium(III) and thulium(III). Inorganic Chemistry, 1983, 22, 2388-2392.	4.0	48
83	Elevation of myoinositol is associated with disease containment in progressive multifocal leukoencephalopathy. Neurology, 2004, 63, 897-900.	1.1	48
84	Keyhole chemical exchange saturation transfer. Magnetic Resonance in Medicine, 2012, 68, 1228-1233.	3.0	48
85	CESTâ€Đixon for human breast lesion characterization at 3 T: A preliminary study. Magnetic Resonance in Medicine, 2018, 80, 895-903.	3.0	48
86	Interrater Reliability in Assessing Quality of Diagnostic Accuracy Studies Using the QUADAS Tool. Academic Radiology, 2006, 13, 803-810.	2.5	47
87	Integrated MR imaging and spectroscopy with chemical shift imaging of P-31 at 1.5 T: initial clinical experience Radiology, 1988, 169, 201-206.	7.3	46
88	Fat suppression by section-select gradient reversal on spin-echo MR imaging. Work in progress Radiology, 1988, 168, 493-495.	7.3	46
89	Cervical carcinoma: MR imaging with an endorectal surface coil Radiology, 1991, 180, 91-95.	7.3	46
90	Investigation of Central Nervous System Dysfunction in Chronic Pelvic Pain Using Magnetic Resonance Spectroscopy and Noninvasive Brain Stimulation. Pain Practice, 2015, 15, 423-432.	1.9	45

#	Article	IF	CITATIONS
91	A nuclear magnetic resonance study of the self-association of adriamycin and daunomycin in aqueous solution. Canadian Journal of Chemistry, 1985, 63, 1233-1238.	1.1	44
92	Accurate Prostate Volume Estimation Using Multifeature Active Shape Models on T2-weighted MRI. Academic Radiology, 2011, 18, 745-754.	2.5	44
93	Simultaneous PML-IRIS after discontinuation of natalizumab in a patient with MS. Neurology, 2012, 78, 1390-1393.	1.1	43
94	Humoral Bone Morphogenetic Protein 2 Is Sufficient for Inducing Breast Cancer Microcalcification. Molecular Imaging, 2008, 7, 7290.2008.00018.	1.4	42
95	Interaction of gadoliniumâ€based MR contrast agents with choline: Implications for MR spectroscopy (MRS) of the breast. Magnetic Resonance in Medicine, 2009, 61, 1286-1292.	3.0	42
96	Metabolic profile of PML lesions in patients with and without IRIS. Neurology, 2012, 79, 1041-1048.	1.1	40
97	Mechanisms of Action of Liraglutide in Patients With Type 2 Diabetes Treated With High-Dose Insulin. Journal of Clinical Endocrinology and Metabolism, 2016, 101, 1798-1806.	3.6	40
98	Proton Spectroscopy in Asymptomatic HIV-Infected Adults: Initial Results in a Prospective Cohort Study. Journal of Acquired Immune Deficiency Syndromes, 1996, 13, 247-253.	0.3	39
99	Perfusion imaging with a freely diffusible hyperpolarized contrast agent. Magnetic Resonance in Medicine, 2011, 66, 746-755.	3.0	38
100	Experimental radiation injury: combined MR imaging and spectroscopy Radiology, 1988, 169, 305-309.	7.3	37
101	Geometric Distortion in Diffusion-weighted MR Imaging of the Prostate—Contributing Factors and Strategies for Improvement. Academic Radiology, 2014, 21, 817-823.	2.5	37
102	Comparison of prostate cancer detection at 3-T MRI with and without an endorectal coil: A prospective, paired-patient study. Urologic Oncology: Seminars and Original Investigations, 2016, 34, 255.e7-255.e13.	1.6	37
103	Mercury-199 nuclear magnetic resonance relaxation in some mercury(II) compounds. Canadian Journal of Chemistry, 1982, 60, 2113-2117.	1.1	36
104	Addressing metabolic heterogeneity in clear cell renal cell carcinoma with quantitative Dixon MRI. JCI Insight, 2017, 2, .	5.0	36
105	Pulmonary vasculature: high-resolution MR imaging. Work in progress Radiology, 1989, 171, 391-395.	7.3	35
106	MR imaging of the pelvis with an endorectal-external multicoil array. Journal of Magnetic Resonance Imaging, 1992, 2, 229-232.	3.4	35
107	The effect of N-acetylaspartate on the intracellular free calcium concentration in NTera2-neurons. Neuroscience Letters, 1995, 198, 209-212.	2.1	35
108	High-Resolution ¹ H NMR Spectroscopy Following Experimental Brain Trauma. Journal of Neurotrauma, 1997, 14, 441-449.	3.4	35

#	Article	IF	CITATIONS
109	MRI of the Placenta Accreta Spectrum (PAS) Disorder: Radiomics Analysis Correlates With Surgical and Pathological Outcome. Journal of Magnetic Resonance Imaging, 2020, 51, 936-946.	3.4	35
110	Carbon magnetic resonance. Signal assignment by alternately pulsed nuclear magnetic resonance and lanthanide-induced chemical shifts. Journal of the American Chemical Society, 1971, 93, 4295-4297.	13.7	34
111	A simple method for processing NMR spectra in which acquisition is delayed: Applications toin vivo localized31P NMR spectra acquired using the DRESS technique. Magnetic Resonance in Medicine, 1988, 7, 88-94.	3.0	34
112	A design for a double-tuned birdcage coil for use in an integrated MRI/MRS examination. Journal of Magnetic Resonance, 1990, 89, 41-50.	0.5	34
113	Localized Proton Spectroscopy without Water Suppression: Removal of Gradient Induced Frequency Modulations by Modulus Signal Selection. Journal of Magnetic Resonance, 2002, 154, 53-59.	2.1	34
114	Proton Magnetic Resonance Spectroscopic Evidence of Glial Effects of Cumulative Lead Exposure in the Adult Human Hippocampus. Environmental Health Perspectives, 2007, 115, 519-523.	6.0	34
115	Sodium MRI of a Human Transplanted Kidney. Academic Radiology, 2009, 16, 886-889.	2.5	34
116	Dynamic Contrast-Enhanced MR Imaging in the Evaluation of Patients with Prostate Cancer. Magnetic Resonance Imaging Clinics of North America, 2009, 17, 363-383.	1.1	34
117	Microstructural correlates of 3D steadyâ€state inhomogeneous magnetization transfer (ihMT) in the human brain white matter assessed by myelin water imaging and diffusion tensor imaging. Magnetic Resonance in Medicine, 2018, 80, 2402-2414.	3.0	34
118	A multisite model for lanthanide shift reagent coordination to monofunctional substrates. Effects of rotational and site averaging on shifts and relaxation rates. Journal of the American Chemical Society, 1976, 98, 4065-4068.	13.7	33
119	Studies of the binding of calcium and lanthanum ions to D-lyxose and D-ribose in aqueous solutions using proton magnetic resonance. Journal of the American Chemical Society, 1976, 98, 3089-3094.	13.7	33
120	Prostate Postbrachytherapy Seed Distribution: Comparison of High-Resolution, Contrast-Enhanced, T1- and T2-Weighted Endorectal Magnetic Resonance Imaging Versus Computed Tomography: Initial Experience. International Journal of Radiation Oncology Biology Physics, 2007, 69, 70-78.	0.8	33
121	Embolization therapy for benign prostatic hyperplasia: Influence of embolization particle size on gland perfusion. Journal of Magnetic Resonance Imaging, 2013, 38, 380-387.	3.4	33
122	Effects of acute ethanol intoxication on experimental brain injury in the rat: neurobehavioral and phosphorus-31 nuclear magnetic resonance spectroscopy studies. Journal of Neurosurgery, 1995, 82, 813-821.	1.6	32
123	Decreases in free cholesterol and fatty acid unsaturation in renal cell carcinoma demonstrated by breath-hold magnetic resonance spectroscopy. American Journal of Physiology - Renal Physiology, 2005, 288, F637-F641.	2.7	32
124	Contact vs. pseudocontact contributions to lanthanide-induced shifts in the nuclear magnetic resonance spectra of isoquinoline and of endo-norbornenol. Journal of the American Chemical Society, 1976, 98, 4250-4258.	13.7	31
125	Silencing of Phosphonate-Gadolinium Magnetic Resonance Imaging Contrast by Hydroxyapatite Binding. Investigative Radiology, 2003, 38, 750-760.	6.2	31
126	Tissue-print and print-phoresis as platform technologies for the molecular analysis of human surgical specimens: mapping tumor invasion of the prostate capsule. Nature Medicine, 2005, 11, 95-101.	30.7	31

#	Article	IF	CITATIONS
127	Conformation of angiotensin II. Evidence for a specific hydrogen bonded conformation. Biochemistry, 1981, 20, 3122-3126.	2.5	29
128	The binding of ytterbium(III) to adriamycin. A proton NMR relaxation study. Journal of the American Chemical Society, 1984, 106, 6905-6909.	13.7	29
129	Brain pH in head injury: An image-guided31P magnetic resonance spectroscopy study. Annals of Neurology, 1990, 28, 661-667.	5.3	28
130	The effect of dietary protein depletion on hepatic 5-Fluorouracil metabolism. Cancer, 1993, 72, 3715-3722.	4.1	28
131	High-resolution anatomic, diffusion tensor, and magnetization transfer magnetic resonance imaging of the optic chiasm at 3T. Journal of Magnetic Resonance Imaging, 2005, 22, 302-306.	3.4	28
132	On shimming approaches in 3T breast MRI. Magnetic Resonance in Medicine, 2013, 69, 862-867.	3.0	28
133	Distortion correction in diffusionâ€weighted imaging of the breast: Performance assessment of prospective, retrospective, and combined (prospective + retrospective) approaches. Magnetic Resonanc in Medicine, 2017, 78, 247-253.	e 3 . 0	28
134	Proton MRS and Neuropsychological Correlates in AIDS Dementia Complex: Evidence of Subcortical Specificity. Journal of Neuropsychiatry and Clinical Neurosciences, 2007, 19, 283-292.	1.8	28
135	An automated algorithm for combining multivoxel MRS data acquired with phased-array coils. Journal of Magnetic Resonance Imaging, 2005, 21, 317-322.	3.4	27
136	An illustration of the potential for mapping MRI/MRS parameters with genetic over-expression profiles in human prostate cancer. Magnetic Resonance Materials in Physics, Biology, and Medicine, 2008, 21, 411-421.	2.0	27
137	The role of magnetic resonance imaging (MRI) in prostate cancer imaging and staging at 1.5 and 3 Tesla: The Beth Israel Deaconess Medical Center (BIDMC) approach. Cancer Biomarkers, 2008, 4, 251-262.	1.7	27
138	Integrating structural and functional imaging for computer assisted detection of prostate cancer on multi-protocol in vivo 3 Tesla MRI. Proceedings of SPIE, 2009, 7260, 72603I.	0.8	27
139	Novel PCA-VIP scheme for ranking MRI protocols and identifying computer-extracted MRI measurements associated with central gland and peripheral zone prostate tumors. Journal of Magnetic Resonance Imaging, 2015, 41, 1383-1393.	3.4	27
140	Lanthanide induced NMR perturbations of hew lysozyme: Evidence for nonaxial symmetry. Biochemical and Biophysical Research Communications, 1977, 76, 711-719.	2.1	26
141	Ionophoric properties of angiotensin II peptides. Nuclear magnetic resonance kinetic studies of the hormone-mediated transport of manganese ions across phosphatidylcholine bilayers. Biochemistry, 1980, 19, 3430-3434.	2.5	26
142	Integrated magnetic resonance imaging and phosphorus spectroscopy of soft tissue tumors. Cancer, 1991, 67, 1849-1858.	4.1	26
143	Bilateral imaging using separate interleaved 3D volumes and dynamically switched multiple receive coil arrays. Magnetic Resonance in Medicine, 1998, 39, 108-115.	3.0	26
144	Fast imaging of phosphocreatine using a RARE pulse sequence. Magnetic Resonance in Medicine, 1998, 39, 851-854.	3.0	26

#	Article	IF	CITATIONS
145	A Comprehensive Segmentation, Registration, and Cancer Detection Scheme on 3 Tesla In Vivo Prostate DCE-MRI. Lecture Notes in Computer Science, 2008, 11, 662-669.	1.3	26
146	Technical Advancements in MR Neurography. Seminars in Musculoskeletal Radiology, 2015, 19, 086-093.	0.7	26
147	Humoral bone morphogenetic protein 2 is sufficient for inducing breast cancer microcalcification. Molecular Imaging, 2008, 7, 175-86.	1.4	26
148	Proton NMR study of iron(II)-bleomycin: Assignment of resonances by saturation transfer experiments. Biochemical and Biophysical Research Communications, 1980, 96, 341-349.	2.1	25
149	Synthetic peptide analogs of skeletal troponin C: Fluorescence studies of analogs of the low-affinity calcium-binding site II. Archives of Biochemistry and Biophysics, 1983, 220, 530-540.	3.0	25
150	Combined MR Imaging and Spectroscopy of Bone and Soft Tissue Tumors. Journal of Computer Assisted Tomography, 1990, 14, 1-10.	0.9	25
151	Principal Component Analysis of Dynamic Contrast Enhanced MRI in Human Prostate Cancer. Investigative Radiology, 2010, 45, 174-181.	6.2	25
152	Zâ€spectrum appearance and interpretation in the presence of fat: Influence of acquisition parameters. Magnetic Resonance in Medicine, 2018, 79, 2731-2737.	3.0	25
153	Texture analysis of magnetic resonance images of the human placenta throughout gestation: A feasibility study. PLoS ONE, 2019, 14, e0211060.	2.5	25
154	Paramagnetic ion induced perturbations in the proton NMR spectrum of lysozyme: a reassignment of the tryptophan indole NH resonances. Journal of the American Chemical Society, 1979, 101, 3071-3077.	13.7	24
155	Proton MR Spectroscopy of Experimental Radiation-Induced White Matter Injury. Journal of Computer Assisted Tomography, 1992, 16, 543-548.	0.9	24
156	A Technique to Identify Isoattenuating Gallstones with Dual-Layer Spectral CT: An ex Vivo Phantom Study. Radiology, 2019, 292, 400-406.	7.3	24
157	Molybdenum-95 nuclear magnetic resonance studies of Molybdenum-phosphorus compounds. Polyhedron, 1982, 1, 130-132.	2.2	23
158	Localized 31P magnetic resonance spectroscopy of large pediatric brain tumors. Journal of Neurosurgery, 1990, 72, 65-70.	1.6	23
159	RF tumour ablation: Computer simulation and mathematical modelling of the effects of electrical and thermal conductivity. International Journal of Hyperthermia, 2005, 21, 199-213.	2.5	23
160	Selective spectroscopic imaging of hyperpolarized pyruvate and its metabolites using a singleâ€echo variable phase advance method in balanced SSFP. Magnetic Resonance in Medicine, 2016, 76, 1102-1115.	3.0	23
161	UCEPR: Ultrafast localized CEST-spectroscopy with PRESS in phantoms and in vivo. Magnetic Resonance in Medicine, 2016, 75, 1875-1885.	3.0	23
162	An NMR investigation of the kinetics of dissociation of the zinc(II) complex of bleomycin antibiotics. Journal of the American Chemical Society, 1979, 101, 5902-5906.	13.7	22

#	Article	IF	CITATIONS
163	Solid-state phosphorus-31 cross-polarization magic-angle spinning NMR study of phosphine complexes of mercury(II). Inorganic Chemistry, 1986, 25, 3202-3204.	4.0	22
164	Magnetic Resonance Imaging and Spectroscopy of Regional Brain Structure in a 10-Year-Old Boy With Elevated Blood Lead Levels. Pediatrics, 1998, 101, e7-e7.	2.1	22
165	MR Imaging of Sodium in the Human Brain with a Fast Three-Dimensional Gradient-Recalled-Echo Sequence at 4 T. Academic Radiology, 2003, 10, 358-365.	2.5	22
166	Accelerating chemical exchange saturation transfer <scp>MRI</scp> with parallel blind compressed sensing. Magnetic Resonance in Medicine, 2019, 81, 504-513.	3.0	22
167	Interactions of gallium(III) with bleomycin antibiotics. Journal of the American Chemical Society, 1980, 102, 131-135.	13.7	21
168	The use of magnetic resonance imaging and spectroscopy in the assessment of patients with head and neck and other superficial human malignancies. Cancer, 1989, 64, 2069-2075.	4.1	21
169	Frame-by-frame PRESS1H-MRS of the brain at 3 T: The effects of physiological motion. Magnetic Resonance in Medicine, 2004, 51, 184-187.	3.0	21
170	Dual-layer spectral detector CT: non-inferiority assessment compared to dual-source dual-energy CT in discriminating uric acid from non-uric acid renal stones ex vivo. Abdominal Radiology, 2018, 43, 3075-3081.	2.1	21
171	Does Tumor FDG-PET Avidity Represent Enhanced Glycolytic Metabolism in Non-Small Cell Lung Cancer?. Annals of Thoracic Surgery, 2020, 109, 1019-1025.	1.3	21
172	Interpretation of the pseudocontact model for nuclear magnetic resonance shift reagents. V. Collinearity in the structural elucidation of nitriles. Journal of the American Chemical Society, 1973, 95, 6846-6848.	13.7	20
173	High-resolution solid-state MAS spectra of 29Si, 27Al, 11B, and other nuclei in inorganic systems using a narrow-bore 400-MHz high-resolution NMR spectrometer. Journal of Magnetic Resonance, 1982, 47, 168-173.	0.5	20
174	Limits on activation-induced temperature and metabolic changes in the human primary visual cortex. Magnetic Resonance in Medicine, 2006, 56, 348-355.	3.0	20
175	Clinical application of pharmacokinetic analysis as a biomarker of solitary pulmonary nodules: Dynamic contrastâ€enhanced MR imaging. Magnetic Resonance in Medicine, 2012, 68, 1614-1622.	3.0	19
176	Quantitative diffusionâ€weighted imaging and dynamic contrastâ€enhanced characterization of the index lesion with multiparametric MRI in prostate cancer patients. Journal of Magnetic Resonance Imaging, 2017, 45, 908-916.	3.4	19
177	Transient MRI enhancement in a patient with seizures and previously resected glioma: Use of MRS. Neurology, 1999, 53, 211-211.	1.1	19
178	Gallium-71 and phosphorus-31 nuclear magnetic resonance studies of the interactions of gallium with phosphoric acid in aqueous solution. Journal of the American Chemical Society, 1978, 100, 5383-5386.	13.7	18
179	The conformation of angiotensin II in solution. III. An analysis of Gd3+-induced perturbations of the 1H nmr spectrum. Journal of Inorganic Biochemistry, 1981, 15, 95-111.	3.5	18
180	Fast imaging of phosphocreatine in the normal human myocardium using a three-dimensional RARE pulse sequence at 4 Tesla. Journal of Magnetic Resonance Imaging, 2002, 15, 467-472.	3.4	18

#	Article	IF	CITATIONS
181	A dose- and time-controllable syngeneic animal model of breast cancer microcalcification. Breast Cancer Research and Treatment, 2010, 122, 87-94.	2.5	18
182	Impact of nonrigid motion correction technique on pixelâ€wise pharmacokinetic analysis of freeâ€breathing pulmonary dynamic contrastâ€enhanced MR imaging. Journal of Magnetic Resonance Imaging, 2011, 33, 968-973.	3.4	18
183	pCEST: Positive contrast using Chemical Exchange Saturation Transfer. Journal of Magnetic Resonance, 2012, 215, 64-73.	2.1	18
184	Criteria and algorithms for the characterization of weak molecular complexes of 2:1 stoichiometry from nuclear magnetic resonance data. Applications to a shift reagent system. Journal of Magnetic Resonance, 1978, 32, 367-376.	0.5	17
185	Proton NMR investigation of Ln3+ complexes of thymopoietin32–36. Biochimica Et Biophysica Acta (BBA) - Protein Structure, 1981, 671, 50-60.	1.7	17
186	An automated iterative algorithm for the quantitative analysis ofin vivo spectra based on the simplex optimization method. Magnetic Resonance in Medicine, 1989, 10, 338-348.	3.0	17
187	High spatial resolution MRI and proton MRS of human frontal cortex. , 1996, 9, 297-304.		17
188	Calcium(II) and the trivalent lanthanide ion complexes of the bleomycin antibiotics. Potentiometric, fluorescence and proton NMR studies. Journal of the American Chemical Society, 1980, 102, 7088-7093.	13.7	16
189	Enhanced multi-protocol analysis via intelligent supervised embedding (EMPrAvISE): detecting prostate cancer on multi-parametric MRI. Proceedings of SPIE, 2011, 7963, 79630U.	0.8	16
190	Gadolinium Retention and Deposition Revisited: How the Chemical Properties of Gadolinium-based Contrast Agents and the Use of Animal Models Inform Us about the Behavior of These Agents in the Human Brain. Radiology, 2017, 285, 721-724.	7.3	16
191	Concentration-dependent Early Antivascular and Antitumor Effects of Itraconazole in Non–Small Cell Lung Cancer. Clinical Cancer Research, 2020, 26, 6017-6027.	7.0	16
192	An analysis of the cobalt(2+) ion-induced nuclear magnetic resonance perturbations of hen egg white lysozyme. Biochemistry, 1978, 17, 1463-1468.	2.5	15
193	Water Modeled Signal Removal and Data Quantification in Localized MR Spectroscopy Using a Time-Scale Postacquistion Method. Journal of Magnetic Resonance, 2001, 149, 45-51.	2.1	15
194	In vivo proton spectroscopy without solvent suppression. Concepts in Magnetic Resonance, 2001, 13, 260-275.	1.3	15
195	Choline Autoradiography of Human Prostate Cancer Xenograft: Effect of Castration. Molecular Imaging, 2008, 7, 7290.2008.00018.	1.4	15
196	Carbon-13 Fourier transform nuclear magnetic resonance study of gallium citrate in aqueous solution. Journal of the American Chemical Society, 1977, 99, 5858-5863.	13.7	14
197	The interactions of gallium with various buffers and chelating agents in aqueous solution: Gallium-71 and hydrogen-1 NMR studies. Bioinorganic Chemistry, 1978, 8, 11-19.	1.1	14
198	The conformation of angiotensin II. Biochimica Et Biophysica Acta (BBA) - Protein Structure, 1981, 667, 157-167.	1.7	14

#	Article	IF	CITATIONS
199	Low-to-high b value DWI ratio approaches in multiparametric MRI of the prostate: feasibility, optimal combination of b values, and comparison with ADC maps for the visual presentation of prostate cancer. Quantitative Imaging in Medicine and Surgery, 2018, 8, 557-567.	2.0	14
200	Line broadenings induced by lanthanide shift reagents: Concentration, frequency, and temperature effects. Journal of Magnetic Resonance, 1976, 21, 47-56.	0.5	13
201	Inhibition of lysozyme by polyvalent metal ions. Biochimica Et Biophysica Acta - Biomembranes, 1978, 527, 56-62.	2.6	13
202	Renal imaging studies at 1.5 and 9.4 T: Effects of diuretics. Magnetic Resonance in Medicine, 1988, 7, 117-124.	3.0	13
203	The correction of nonuniform signal intensity profiles in magnetic resonance imaging. Journal of Digital Imaging, 1989, 2, 2-8.	2.9	13
204	31P Localized Magnetic Resonance Spectroscopy of Head and Neck Tumors—Preliminary Findings. Otolaryngology - Head and Neck Surgery, 1990, 103, 775-783.	1.9	13
205	1H N.M.R. STUDY OF THE CONFORMATION OF [Glu 4] OXYTOCIN AND ITS LANTHANIDE COMPLEXES IN AQUEOUS SOLUTION. International Journal of Peptide and Protein Research, 1981, 17, 56-64.	0.1	12
206	Separating High-Z Oral Contrast From Intravascular Iodine Contrast in an Animal Model Using Dual-Layer Spectral CT. Academic Radiology, 2019, 26, 1237-1244.	2.5	12
207	A fluorescence study of the binding of calcium and terbium ions to angiotensin. Bioinorganic Chemistry, 1978, 8, 363-368.	1.1	11
208	The use of T2 distribution to study tumor extent and heterogeneity in head and neck cancer. Magnetic Resonance Imaging, 1991, 9, 205-211.	1.8	11
209	Yb-DTPA, a novel contrast agent in magnetic resonance imaging: Application to rat kidney. Magnetic Resonance in Medicine, 1991, 17, 328-335.	3.0	11
210	InÂVitro MR Imaging of Renal Stones with an Ultra-short Echo Time Magnetic Resonance Imaging Sequence. Academic Radiology, 2012, 19, 1566-1572.	2.5	11
211	Ultrashort echo time MRI of pulmonary water content: assessment in a sponge phantom at 1.5 and 3.0 Tesla. Diagnostic and Interventional Radiology, 2013, 20, 34-41.	1.5	11
212	An iterative deconvolution algorithm for image recovery in clinical CT: A phantom study. Physica Medica, 2015, 31, 903-911.	0.7	11
213	Pseudoenhancement effects on iodine quantification from dual-energy spectral CT systems: A multi-vendor phantom study regarding renal lesion characterization. European Journal of Radiology, 2018, 105, 125-133.	2.6	11
214	Clinical Magnetic Resonance Spectroscopy:. Investigative Radiology, 1989, 24, 1034-1038.	6.2	10
215	Prostatome: A combined anatomical and disease based MRI atlas of the prostate. Medical Physics, 2014, 41, 072301.	3.0	10
216	How the Chemical Properties of GBCAs Influence Their Safety Profiles In Vivo. Molecules, 2022, 27, 58.	3.8	10

#	Article	IF	CITATIONS
217	Nuclear magnetic resonance analysis of Gd3+-induced perturbations in thymopoietin32–36: A study of amide and aromatic proton resonances. Archives of Biochemistry and Biophysics, 1982, 217, 468-472.	3.0	9
218	COLLINARUS: collection of image-derived non-linear attributes for registration using splines. , 2009, , .		9
219	Empirical evaluation of bias field correction algorithms for computer-aided detection of prostate cancer on T2w MRI. , 2011, , .		9
220	Balanced Steady-State Free Precession (bSSFP) from an effective field perspective: Application to the detection of chemical exchange (bSSFPX). Journal of Magnetic Resonance, 2017, 275, 55-67.	2.1	9
221	Phantom Validation of Spectral Detector Computed Tomography–Derived Virtual Monoenergetic, Virtual Noncontrast, and Iodine Quantification Images. Journal of Computer Assisted Tomography, 2018, 42, 959-964.	0.9	9
222	Lanthanide Complexes of Peptides and Proteins. , 1984, , 23-71.		9
223	NMR relaxation studies of 103Rh. Journal of Magnetic Resonance, 1982, 46, 168-171.	0.5	8
224	A conformational analysis of adriamycin based upon its 1H nuclear magnetic resonance spectrum in various solvents. Canadian Journal of Chemistry, 1987, 65, 2405-2410.	1.1	8
225	Adriamycin Complexes of Pd(II) and Pt(II). Journal of Inorganic Biochemistry, 1987, 30, 35-43.	3.5	8
226	Magnetic Resonance Imaging and Magnetic Resonance Spectroscopy of Bone Tumors and Bone Marrow Disease. Investigative Radiology, 1989, 24, 1006-1010.	6.2	8
227	High-Resolution Computed Tomography of Single Breast Cancer Microcalcifications in Vivo. Molecular Imaging, 2011, 10, 7290.2010.00050.	1.4	8
228	Wholeâ€body MRI for metastatic cancer detection using T ₂ â€weighted imaging with fat and fluid suppression. Magnetic Resonance in Medicine, 2018, 80, 1402-1415.	3.0	8
229	Localization in Clinical NMR Spectroscopy. Biological Magnetic Resonance, 1992, , 1-53.	0.4	8
230	The nature of the Ln3+ —angiotensin II complex. A 13C nmr study of the binding of Yb3+ to angiotensin ii. Journal of Inorganic Biochemistry, 1983, 18, 175-180.	3.5	7
231	Lanthanide complexes of adriamycin. Journal of the Less Common Metals, 1983, 94, 359-365.	0.8	7
232	The thermodynamics of lanthanide ion binding to adriamycin. Journal of Inorganic Biochemistry, 1985, 24, 59-67.	3.5	7
233	Initial Experience with Fast Low-Angle Multiecho (FLAME) Imaging of the Central Nervous System. Journal of Computer Assisted Tomography, 1988, 12, 171-174.	0.9	7
234	Use of Spectral Detector Computed Tomography to Improve Liver Segmentation and Volumetry. Journal of Computer Assisted Tomography, 2020, 44, 197-203.	0.9	7

#	Article	IF	CITATIONS
235	N-acetylaspartate complexes with calcium and lanthanide ions. Journal of Inorganic Biochemistry, 1995, 60, 31-43.	3.5	6
236	Gadolinium Deposition and Retention in the Brain: Should We Be Concerned?. Radiology: Cardiothoracic Imaging, 2019, 1, e190104.	2.5	6
237	Combining inhomogeneous magnetization transfer and multipoint Dixon acquisition: Potential utility and evaluation. Magnetic Resonance in Medicine, 2021, 85, 2136-2144.	3.0	6
238	Reaction of Gibbs reagent (2,6-dichlorobenzoquinone 4-chloroimine) with the antioxidant BHA (3-tertbutyl 4-hydroxyanisole): isolation and identification of the major product. Journal of Chromatography A, 1984, 294, 375-379.	3.7	5
239	Complementary roles of PET and MR spectroscopy in the management of brain tumors Radiology, 1990, 177, 617-618.	7.3	5
240	MR Spectroscopy. Academic Radiology, 2001, 8, 567-570.	2.5	5
241	Statistical 3D prostate imaging atlas construction via anatomically constrained registration. , 2013, 8669, .		5
242	Neurochemical Changes Observed by InÂVivo Proton Magnetic Resonance Spectroscopy in the Mouse Brain Postadministration of Scopolamine. Academic Radiology, 2014, 21, 1072-1077.	2.5	5
243	<title>In vivo imaging of small animals with optical tomography and near-infrared fluorescent probes</title> . , 2002, , .		4
244	Optimal breathing protocol for dynamic contrast-enhanced MRI of solitary pulmonary nodules at 3T. European Journal of Radiology, 2007, 64, 397-400.	2.6	4
245	Remission of progressive multifocal leukoencephalopathy and primary central nervous system lymphoma in an HIV-infected patient. European Journal of Neurology, 2007, 14, 598-602.	3.3	4
246	MRI contrast using solidâ€state, <i>B</i> ₁ â€distorting, microelectromechanical systems (MEMS) microresonant devices (MRDs). Magnetic Resonance in Medicine, 2009, 61, 860-866.	3.0	4
247	A structural-functional MRI-based disease atlas: application to computer-aided-diagnosis of prostate cancer. Proceedings of SPIE, 2010, , .	0.8	4
248	Integrating an adaptive region-based appearance model with a landmark-free statistical shape model: application to prostate MRI segmentation. , 2011, , .		4
249	Phantom and Preclinical Studies for Image Improvement in Clinical CT. IEEE Transactions on Radiation and Plasma Medical Sciences, 2019, 3, 96-102.	3.7	4
250	Integrated MR imaging and proton nuclear magnetic resonance spectroscopy in a family with an X-linked spastic paraparesis. American Journal of Neuroradiology, 1991, 12, 785-9.	2.4	4
251	Investigating new CT contrast agents: a phantom study exploring quantification and differentiation methods for high-Z elements using dual-energy CT. European Radiology, 2021, 31, 8060-8067.	4.5	3
252	A 1H NMR study of the reaction of adriamycin with Pd(II). Inorganica Chimica Acta, 1987, 136, L21-L24.	2.4	2

#	Article	IF	CITATIONS
253	Noise reduction for T2 derived magnetic resonance images. Computerized Medical Imaging and Graphics, 1990, 14, 185-190.	5.8	2
254	WERITAS: weighted ensemble of regional image textures for ASM segmentation. , 2009, , .		2
255	The role of magnetic resonance imaging in prostate cancer imaging and staging. , 2011, , .		2
256	Science to Practice: Can Hyperpolarized Water Be Used to Enhance MR Angiography and Flow Measurement?. Radiology, 2012, 265, 325-326.	7.3	2
257	Quantification of Mouse Renal Perfusion Using Arterial Spin Labeled MRI at 1 T. Academic Radiology, 2017, 24, 1079-1085.	2.5	2
258	Breast Tumor Microcalcification Induced by Bone Morphogenetic Protein-2: A New Murine Model for Human Breast Tumor Diagnosis. Contrast Media and Molecular Imaging, 2018, 2018, 1-9.	0.8	2
259	The Lanthanides as Structural Probes in Peptides. , 1982, , 45-51.		2
260	Dementias and Neuroimaging. Academic Radiology, 2008, 15, 1087-1088.	2.5	1
261	MR spectroscopy in translational neuroscience. Journal of Comparative Neurology, 2010, 518, 4089-4090.	1.6	1
262	Dedicated PET device for breast PET and MRI/PET correlations. European Journal of Radiology, 2012, 81, S149-S150.	2.6	1
263	Image improvement method for positron emission mammography. Physica Medica, 2017, 39, 164-173.	0.7	1
264	Spatial Resolution versus Reproducibility for Dynamic MRI of High-Grade Gliomas. Radiology, 2021, 300, 421-422.	7.3	1
265	MR Spectroscopy. , 2005, , 115-127.		1
266	Improving the Accuracy of Screening Dense Breasted Women for Breast Cancer By Combining Clinically Based Risk Assessment Models with Ultrasound Imaging. Academic Radiology, 2022, 29, S8-S9.	2.5	1
267	Image enhancement method for digital mammography. , 2018, , .		1
268	High resolution nuclear magnetic resonance (NMR) studies of cation transport across model and living biological membranes: aqueous shift reagents for 23Na, 39K and 25Mg NMR. Journal of the Less Common Metals, 1983, 94, 408.	0.8	0
269	Hydrogen ultrathin phase-encoded spectroscopy (HUPSPEC). Magnetic Resonance in Medicine, 1990, 14, 507-521.	3.0	0
270	Limitations of magnetic resonance spectroscopy in patients with white matter disease. Annals of Neurology, 1994, 36, 932-932.	5.3	0

#	Article	IF	CITATIONS
271	Proton MRS in first episode patients with schizophrenia: Abnormalities in NAA and CHO ratios to creatine in frontal and temporal lobes. Schizophrenia Research, 1997, 24, 178.	2.0	0
272	Personal diary: A research PhD's perspective. Academic Radiology, 2001, 8, 173-174.	2.5	0
273	Dynamic contrast-enhanced MR studies. Academic Radiology, 2003, 10, 961-962.	2.5	0
274	PARACEST Agents: Modulating MRI Contrast via Water Proton Exchange. ChemInform, 2004, 35, no.	0.0	0
275	In Reply to Drs. Beaulieu and Verhagen. International Journal of Radiation Oncology Biology Physics, 2008, 71, 1289-1290.	0.8	0
276	Endoluminal MRI of the Pancreas: A Novel Imaging Technology. Gastrointestinal Endoscopy, 2008, 67, AB132.	1.0	0
277	Hyperpolarized C-13 studies of cancer metabolism in animal models. Hype or real?. European Journal of Radiology, 2012, 81, S85-S86.	2.6	0
278	Iterative multiple reference tissue method for estimating pharmacokinetic parameters on prostate DCE MRI. Proceedings of SPIE, 2013, , .	0.8	0
279	MP16-04 A COMPARISON OF PROSTATE CANCER DETECTION AT 3T MRI WITH AND WITHOUT AN ENDORECTAL COIL: A PROSPECTIVE, PAIRED-PATIENT STUDY. Journal of Urology, 2016, 195, .	0.4	0
280	Image enhancement in positron emission mammography. , 2017, , .		0
281	1696: Mri-Visible Phenotypes of Human Prostate Cancer: Gene Expression Profiles of DCE-MRI Positive Tumors. Journal of Urology, 2007, 177, 563-563.	0.4	0
282	Abstract LB-418: Targeting the PI3K/mTOR pathway in genetically engineered mouse models of prostate cancer. , 2011, , .		0
283	Paramagnetic Metal lons as Nuclear Magnetic Resonance Probes of Peptide Conformation in Solution. , 1985, , 301-353.		0
284	Integrated Magnetic Resonance Imaging and 31P-Magnetic Resonance Spectroscopy of Soft Tissue Masses. , 1990, , 255-269.		0